

Selected Parity Violation Experiments

W. D. RAMSAY

*Department of Physics and Astronomy, University of Manitoba, Winnipeg, MB, R3T
2N2, Canada*

Received 20 October 2003;
final version:

I start by reviewing existing $\vec{p}p$ measurements with particular emphasis on the recent 221 MeV $\vec{p}p$ measurement at TRIUMF which permitted the weak meson-nucleon coupling constants h_{ρ}^{pp} and h_{ω}^{pp} to be determined separately for the first time. I then review $\vec{n}p$ experiments, with specific details of the $\vec{n}p \rightarrow d\gamma$ experiment now under preparation at Los Alamos National Laboratory. This experiment will provide a clean measurement of the weak pion nucleon coupling, f_{π} . Finally, I discuss $\vec{e}p$ parity violation experiments, particularly the Gzero experiment under way at Jefferson Lab in Virginia. This experiment will measure the weak form factors G_E^z and G_M^z , allowing the distribution of strange quarks in the quark sea to be determined.

PACS: 11.30.Er, 24.70.+s, 25.40.Cm, 25.40.Lw, 13.60.Fz

Key words: parity violation, polarized beams, proton, electron, form factor

1 Introduction

In Vancouver a popular form of Chinese luncheon is “Dim Sum” in which small quantities of a large variety of foods may be tasted. This review is a “Dim Sum” of parity violation experiments. As with a luncheon, my selection is biased by my personal taste and experience. I start with $\vec{p}p$ parity violation experiments, concentrating on the the TRIUMF 221 MeV $\vec{p}p$ experiment, then discuss $\vec{n}p$ parity violation experiments with details of the Los Alamos $\vec{n}p \rightarrow d\gamma$ experiment now being installed at LANSCE. Finally, I discuss $\vec{e}p$ parity violation experiments, particularly the Gzero experiment at Jefferson Lab. I refer those interested in more background to specific reviews on nucleon-nucleon [1, 2] and $\vec{e}p$ [3] experiments.

2 $\vec{p}p$ Experiments

Figure 1 shows typical $\vec{p}p$ parity violation experiments. They scatter a longitudinally polarized beam of protons from a hydrogen target and measure the difference in cross section for right-handed and left-handed proton helicities. The intermediate and high energy experiments use transmission geometry in which the change in scattering cross section is deduced from the change in transmission through the target. Low energy experiments, where energy loss limits the target thickness, use scattering geometry, in which the detectors measure the scattered protons directly. Both types of experiments measure the parity violating longitudinal analyzing power, $A_z = \frac{\sigma^+ - \sigma^-}{\sigma^+ + \sigma^-}$, where σ^+ and σ^- are the scattering cross sections for positive and negative helicity.

Table 1. Summary of $\bar{p}p$ parity violation experiments. The long times taken to achieve small uncertainties reflects the time taken to understand and correct for systematic errors. In cases where authors reported both statistical and systematic uncertainties, this table shows the quadrature sum of the two.

Lab/Energy	Technical Details	A_z (10^{-4})	Where Reported
Los Alamos 15 MeV	scattering 3 atm x 38cm hydrogen gas 4 liquid scintillators	$+1 \pm 4$	1974 Phys. Rev. Lett. [4]
	scattering 6.9 atm hydrogen gas 4 plastic scintillators	-1.7 ± 0.8	1978 Argonne Conference [5]
Texas A&M 47 MeV	scattering 39 atm x 42cm hydrogen gas 4 plastic scintillators	-4.6 ± 2.6	1983 Florence Conference [6]
Berkeley 46 MeV	scattering 80 atm hydrogen gas target He ion chamber around target	-1.3 ± 1.1	1980 Santa Fe Conference [7]
SIN (PSI) 45 MeV	scattering 100 atm hydrogen gas annular ion chamber	-1.63 ± 1.03	1985 Osaka Conference [8]
		-3.2 ± 1.1	1980 Phys. Rev. Lett. [9]
		-2.32 ± 0.89	1984 Phys. Rev. D. [10]
		-1.50 ± 0.22	1987 Phys. Rev. Lett. [11]
Los Alamos 800 MeV	transmission 1 m liquid hydrogen gas ion chambers	$+2.4 \pm 1.1$	1986 Phys. Rev. Lett. [12]
Bonn 13.6 MeV	scattering 15 atm hydrogen gas hydrogen ion chambers	-1.5 ± 1.1	1991 Phys. Lett. B [13]
		-0.93 ± 0.21	1994 private communication [14]
TRIUMF 221 MeV	transmission 40 cm liquid hydrogen hydrogen ion chambers	$+0.84 \pm 0.34$	2001 Phys. Rev. Lett. [15]
Argonne ZGS 5130 MeV	transmission 81 cm water target ion chambers and scintillators	$+26.5 \pm 7.0$	1986 Phys. Rev. Lett. [16]

A roughly historical summary of $\bar{p}p$ parity violation experiments is given in Table 1. The long time taken to acquire measurements at a reasonable selection of energies and with small experimental uncertainties reflects the technical difficulty of these measurements. Running time is dominated by the time required to understand, and correct for, the various sources of systematic error. The time required to get the desired statistical precision is normally small by comparison.

The TRIUMF pp experiment [15] is a transmission experiment as shown in the lower panel of figure 1. A 221 MeV longitudinally polarized proton beam was passed through a 400 mm long liquid hydrogen target, which scattered about 4% of the beam. Hydrogen filled ion chambers located upstream and downstream of the tar-

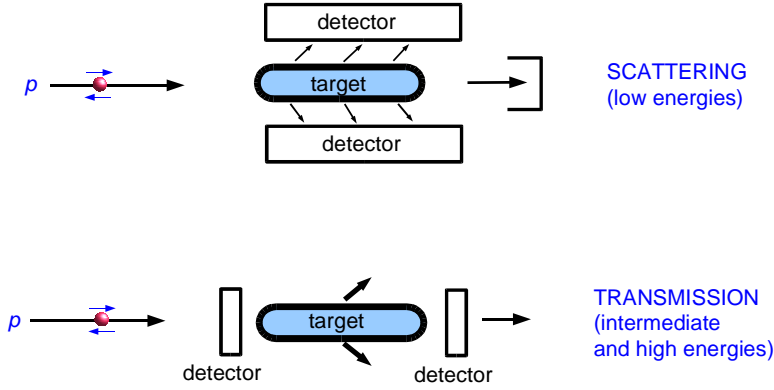


Fig. 1. Types of $\bar{p}p$ experiments. The low-energy experiments use scattering geometry, while the intermediate and high-energy experiments use transmission geometry.

Table 2. Overall corrections for systematic errors in the TRIUMF parity violation experiment. The table shows the average value of each coherent modulation, the net correction made for this modulation, and the uncertainty resulting from applying the correction.

Property	Average Value	$10^7 \Delta A_z$
$A_z^{uncorrected}(10^{-7})$	$1.68 \pm 0.29(stat.)$	
$y * P_x(\mu m)$	-0.1 ± 0.0	-0.01 ± 0.01
$x * P_y(\mu m)$	-0.1 ± 0.0	0.01 ± 0.03
$\langle yP_x \rangle(\mu m)$	1.1 ± 0.4	0.11 ± 0.01
$\langle xP_y \rangle(\mu m)$	-2.1 ± 0.4	0.54 ± 0.06
$\Delta I/I(ppm)$	15 ± 1	0.19 ± 0.02
position + size		0 ± 0.10
$\Delta E(meV at OPPIS)$	7–15	0.0 ± 0.12
electronic crosstalk		0.0 ± 0.04
Total		$0.84 \pm 0.17(syst.)$
$A_z^{corr}(10^{-7})$	$0.84 \pm 0.29(stat.) \pm 0.17(syst.)$	

get measured the change in transmission when the spin of the incident protons was flipped from right-handed to left-handed. Although a very good optically pumped polarized ion source [17, 18, 19] was used that minimized the changes in beam properties other than helicity, other beam properties still changed very slightly. These helicity-correlated beam property changes caused a systematic shift in the A_z distribution, and corrections must be made. To do this, the TRIUMF group continuously measured the helicity correlated changes in beam properties and made corrections based on the sensitivities determined in separate control measurements. All the corrections are summarized in Table 2. The importance of accurate corrections is

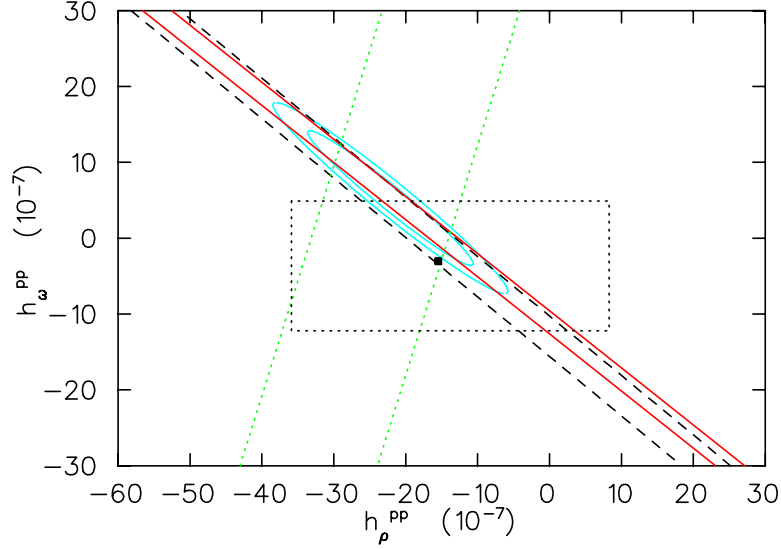


Fig. 2. Constraints on the weak meson-nucleon couplings imposed by experiments in the energy range where the meson exchange model is normally used. The bands are based on calculations by Carlson *et al.* [22] using the AV18 potential [20] and CD-Bonn strong couplings [21]. The contours are 68% and 90% C.L. (Figure modified from [15])

apparent when one notes that the measured raw A_z actually came half from true parity violation and half from false effects.

Because the range of the W and Z bosons carrying the weak force is so small ($\sim 0.002 fm$), the low and intermediate energy $\bar{p}p$ results are normally interpreted using meson exchange models, and parameterized in terms of a set of π , ρ , and ω weak meson-nucleon coupling constants. $\bar{p}p$ experiments are sensitive to the combinations $h_\rho^{pp} = h_\rho^{(0)} + h_\rho^{(1)} + \frac{1}{\sqrt{6}}h_\rho^{(2)}$ and $h_\omega^{pp} = h_\omega^{(0)} + h_\omega^{(1)}$. Where the subscript denotes the exchanged meson and the superscript the isospin change.

The value of the couplings can be extracted from the experiments by assuming a realistic model for the strong interaction and adjusting the weak couplings to fit the data. Using the AV18 strong potential [20] and CD-Bonn values for the strong couplings [21], Carlson *et al.* [22] calculate that

$$\begin{aligned} A_z(13.6MeV) &= 0.059h_\rho^{pp} + 0.075h_\omega^{pp} \\ A_z(45MeV) &= 0.10h_\rho^{pp} + 0.14h_\omega^{pp} \\ A_z(225MeV) &= -0.038h_\rho^{pp} + 0.010h_\omega^{pp} \end{aligned}$$

where the energies correspond to the most accurate measurements over the low and intermediate energy range [11, 14, 15]. These constraints are shown graphically in

Fig. 2. Note that the low energy results scale as \sqrt{E} and hence constrain essentially the same linear combination of h_ρ^{pp} and h_ω^{pp} . It was only when the TRIUMF result became available that h_ρ^{pp} and h_ω^{pp} could be separately determined. By adjusting the couplings for the best fit to the data, Carlson *et al.* [22] estimate $h_\rho^{pp} = -22.3 \times 10^{-7}$ and $h_\omega^{pp} = 5.17 \times 10^{-7}$ compared to the DDH [23] theoretical “best guess” values of $h_\rho^{pp} = -15.5 \times 10^{-7}$ and $h_\omega^{pp} = 3.0 \times 10^{-7}$

3 $\vec{n}p \rightarrow d\gamma$ Experiments

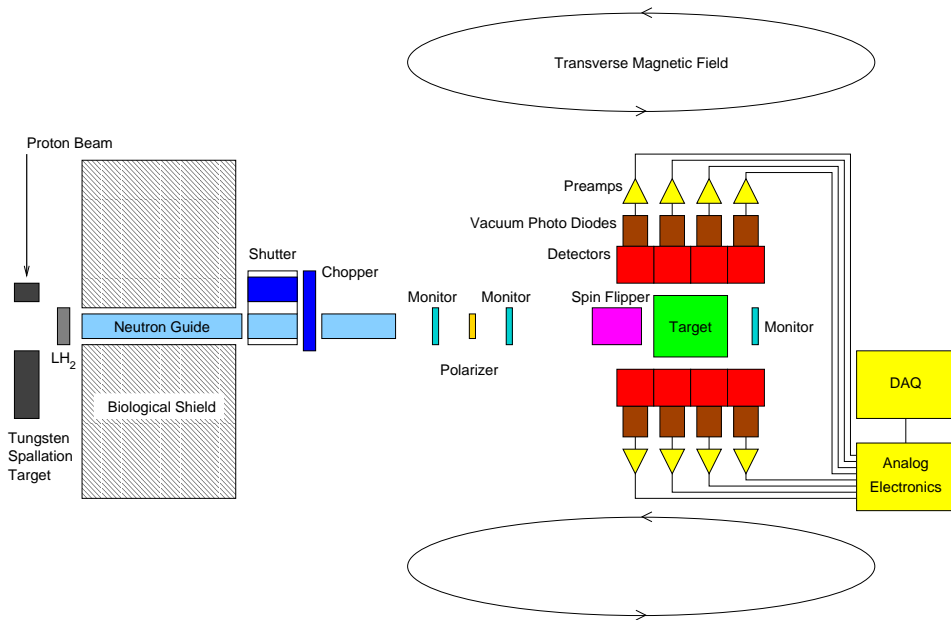


Fig. 3. Layout of apparatus for the $\vec{n}p \rightarrow d\gamma$ experiment at LANSCE.

Unlike the $\vec{p}p$ experiments just discussed, which are sensitive to ρ and ω exchange, $\vec{n}p \rightarrow d\gamma$ experiments are sensitive almost exclusively to pion exchange, and measure the weak pion-nucleon coupling, f_π . In an $\vec{n}p \rightarrow d\gamma$ experiment, the incident cold neutrons are polarized vertically and the gamma rays produced by neutron capture in the hydrogen target are expected to be emitted slightly more in the direction opposite to the neutron spin. The up-down asymmetry $A_\gamma \approx -0.11 f_\pi$ provides a clean measure of f_π ¹⁾ free of nuclear structure uncertainties [24]. Previous measurements at ILL Grenoble gave $A_\gamma = (6 \pm 21) \times 10^{-8}$ [25] and $A_\gamma = (-1.5 \pm 4.8) \times 10^{-8}$ [26], but neither result was accurate enough to impose a significant constraint.

¹⁾ Some authors quote $H_\pi = f_\pi \frac{g_\pi}{\sqrt{32}}$, where g_π is the strong pion-nucleon coupling.

An experiment is now being prepared at Los Alamos to measure the gamma ray asymmetry in $\bar{n}p \rightarrow d\gamma$ with an uncertainty of $\pm 0.5 \times 10^{-8}$ [24]. The expected asymmetry is $A_\gamma \approx -5 \times 10^{-8}$. The apparatus is shown schematically in Fig. 3. Neutrons are produced by an 800 MeV proton beam incident on a tungsten spallation target. The neutrons are cooled in a liquid hydrogen moderator and transported to the experiment through a super mirror neutron guide. The neutrons are polarized vertically by a polarized ^3He spin filter then captured in a liquid para-hydrogen target. The gamma asymmetry is measured by an array of $48 \times 15 \times 15 \text{ cm}^2$ CsI(Tl) detectors surrounding the target.

The neutron beam is pulsed at 20 Hz, so the energy of the neutrons arriving at the experiment after the 22 m flight path can be determined by time of flight. An RF spin flipper provides a method of rapid spin reversal to control systematic errors. Systematic errors can be further understood and controlled by reversing the ^3He cell direction or the direction of the overall vertical 10 gauss guide field. In addition, different systematic errors have different dependences on time of flight.

The beamline, FP12, is now complete and the experimental cave is scheduled for completion in fall, 2003. Commissioning runs will follow, with the first production data taking anticipated in late 2004 and 2005.

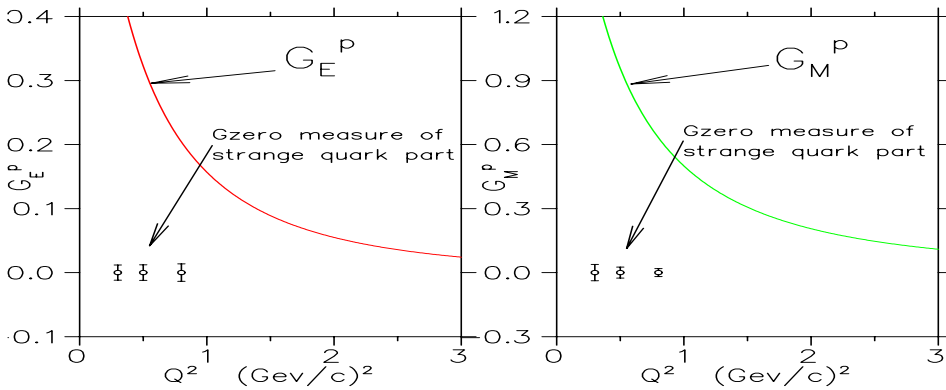


Fig. 4. The proton form factors G_E^p and G_M^p [28] are the sum of contributions from up and down and strange quarks. The points with error bars show the anticipated uncertainty in the Gzero measurement of the strange quark part.

4 $\bar{e}p$ Experiments – The Gzero Experiment

The Gzero experiment [27] at Jefferson Lab scatters a longitudinally polarized electron beam from a 200 mm liquid hydrogen target, and measures the parity-violating longitudinal analyzing power $A_z = \left[\frac{1}{P} \right] \frac{\sigma^R - \sigma^L}{\sigma^R + \sigma^L}$ where σ^R and σ^L are the cross sections for right-handed and left-handed electrons, and P is the beam polarization. A_z values ranging from -3 to -35 ppm are predicted. By measuring

this quantity at a range of angles and momentum transfers, the experiment will determine the *weak* charge and magnetic form factors $G_{E,M}^Z(Q^2)$ (essentially the Fourier transforms of the spatial distributions). Because the weak charges of the quarks are different than the electromagnetic charges (Table 3), one can combine these weak form factors with the previously measured *electromagnetic* form factors $G_{E,M}^{p,\gamma}$ of the proton and $G_{E,M}^{n,\gamma}$ of the neutron and extract the strange quark form factors

$$G_{E,M}^{s,p} = (1 - 4 \sin^2 \theta_W) G_{E,M}^{p,\gamma} - G_{E,M}^{n,\gamma} - G_{E,M}^{p,Z},$$

where θ_W is the weak mixing angle and $G_{E,M}^{p,Z}$ are the proton electroweak form factors to be measured by Gzero. Figure 4 shows the proton form factors G_E^p and G_M^p taken from a fit to the existing parity conserving data [28]. At low Q^2 , where the effective wavelength of the virtual photon probe is very long, the form factors are simply the proton charge and magnetic moment, 1.00 and 2.79. These form factors are the sum of contributions from the different quarks; the points on the graph show the expected error in the Gzero measurement of the strange quark part.

Table 3. Electroweak couplings of up, down, and strange quarks

quark	electric charge	weak charge
u	$+\frac{2}{3}$	$+1 - \frac{4}{3} \sin^2 \theta_W$
d	$-\frac{1}{3}$	$-1 + \frac{2}{3} \sin^2 \theta_W$
s	$-\frac{1}{3}$	$-1 + \frac{2}{3} \sin^2 \theta_W$

The charge and magnetic form factors can be separated by measuring at forward and backward angles. In each configuration, several values of momentum transfer, Q^2 , in the range $0.1 < Q^2 < 1.0 (GeV/c)^2$ will be measured. Do do this, the scattered particles pass through an 8-sector superconducting magnetic spectrometer and are detected by an array of plastic scintillators arranged in contours of constant Q^2 . In the forward configuration protons are detected at $\theta_p = 70^\circ \pm 10^\circ$ (or $\theta_e = 11^\circ \pm 4^\circ$). Over this angular range there is a strong dependence of Q^2 on scattering angle, and only one beam energy of 3 GeV is required for all Q^2 . In the backward configuration, electrons are detected at $\theta_e = 110^\circ \pm 10^\circ$. In this case, Q^2 is only weakly dependent on scattering angle, and the beam energy must be changed for each Q^2 . Beam energies of 424, 585, and 799 MeV, corresponding to Q^2 of 0.3, 0.5, and 0.8 $(GeV/c)^2$ are presently planned for the backward angles.

To extract $G_{E,M}^Z$ a correction must be made for the small contribution of the axial form factor, G_A^e , to the measured A_z . Gzero will determine this experimentally by measuring quasi-elastic back angle scattering from deuterium. By measuring at at both forward and backward angles and with both hydrogen and deuterium targets, Gzero will be able to determine G_E^s , G_M^s , and G_A^s separately. As shown in Table 4, other $\vec{e}p$ experiments have measured, or are planning to measure, various linear combinations of the form factors.

Table 4. Comparison of $\vec{e}p$ parity violation experiments. Depending on the scattering angle and momentum transfer, the experiments are sensitive to different linear combinations of form factors

Experiment	E_{beam}	I_{beam}	θ_e (deg)	Q^2	Target	Observable
SAMPLE [29, 30] (MIT-Bates)	200 MeV	pulsed (2.7 mA peak)	130–160	0.1	LH ₂	$G_M^s + 0.44G_A^s$
					LD ₂	$G_M^s + 2.37G_A^s$
HAPPEX [31, 32] (Jlab Hall-A)	3.3 GeV	35 μ A	12.3	0.477	LH ₂	$G_E^s + 0.39G_M^s$
HAPPEX-2 [33]			6	0.1	LD ₂	$G_E^s + 0.08G_M^s$
He[34]			6	0.1	He	G_E^s
PVA4 [35, 36, 37] (MAMI-Mainz)	854 MeV	20 μ A	35	0.225 0.11	LH ₂	$G_E^s + 0.22G_M^s$ $G_E^s + 0.10G_M^s$
G-zero [27, 38] (Jlab Hall-C)	3 GeV	35 μ A	6-20	0.1-1.0	LH ₂	measurements together give G_E^s, G_M^s and G_A^s
	424 MeV		100–120	0.3	LH ₂	
	576 MeV			0.5		
	799 MeV			0.8		
	424 MeV		100–120	0.3	LD ₂	
	576 MeV			0.5		
799 MeV		0.8				

The Gzero experiment completed a successful commissioning run of the forward angle configuration in fall 2002 and January 2003 and all major systems are now fully operational. Running will continue with an engineering run October to December, 2003, and production running is scheduled to start in 2004.

5 summary

Parity violation experiments provide a way to study effects of the weak interaction in the presence of the much stronger electromagnetic and strong nuclear interactions. The polarized beam experiments I have described use similar experimental techniques and face similar problems controlling systematic errors. The physics addressed by these experiments can, however be quite diverse. $\vec{n}p$ experiments constrain the weak pion-nucleon coupling constant, f_π . $\vec{p}p$ parity violation experiments are sensitive to the shorter range part of the nucleon-nucleon force and constrain the combinations $h_\rho^{pp} = h_\rho^{(0)} + h_\rho^{(1)} + \frac{1}{\sqrt{6}}h_\rho^{(2)}$ and $h_\omega^{pp} = h_\omega^{(0)} + h_\omega^{(1)}$. Finally, $\vec{e}p$ parity violation experiments, such as the Jlab Gzero experiment, offer the opportunity to measure the contribution of strange quark-antiquark pairs to the proton charge and magnetism.

References

- [1] E.G. Adelberger and W.C. Haxton, Ann. Rev. Nucl. Part. Sci. **35**, 501 (1985).

- [2] W. Haeberli and Barry R. Holstein, in *Symmetries and Fundamental Interactions in Nuclei*, edited by W.C. Haxton and E.M. Henley, (World Scientific, 1995) p. 17.
- [3] R.D. McKeown and M.J. Ramsey-Musolf, *Mod. Phys. Lett. A* **18**, 75 (2003); hep-ph/0203011 .
- [4] J.M. Potter *et al.*, *Phys. Rev. Lett.* **33**, 1307 (1974).
- [5] D.E. Nagle *et al.*, in *Proceedings of the 3rd International Conference on High Energy Beams and Polarized Targets* (Argonne, 1978), edited by L.H. Thomas, AIP Conference Proceedings 51, New York 1979, p. 224.
- [6] D.M. Tanner *et al.*, in *Proceedings of the International Conference on Nuclear Physics* (Florence, 1983), (Typographia, Bologna, 1983), p. 697.
- [7] P. von Rossen *et al.*, in *Proceedings of the 5th International Symposium on Polarization Phenomena in Nuclear Physics* (Santa Fe, 1980), edited by G.G. Ohlsen *et al.*, AIP Conference Proceedings 69, New York, 1981, p. 1442.
- [8] P. von Rossen *et al.*, in *Proceedings of the 6th International Symposium on Polarization Phenomena in Nuclear Physics* (Osaka, 1985), *J. Phys. Soc. Japan* **55**, Suppl. p. 1016 (1986).
- [9] R. Balzer *et al.*, *Phys. Rev. Lett.* **44**, 699 (1980).
- [10] R. Balzer *et al.*, *Phys. Rev. C* **30**, 1409 (1984).
- [11] S. Kistryn *et al.*, *Phys. Rev. Lett.* **58**, 1616 (1987).
- [12] V. Yuan *et al.*, *Phys. Rev. Lett.* **57**, 1680 (1986).
- [13] P.D. Eversheim *et al.*, *Phys. Lett. B* **256**, 11 (1991)
- [14] P.D. Eversheim, private communication (1994).
- [15] A.R. Berdoz *et al.*, *Phys. Rev. Lett.* **87**, 272301 (2001).
- [16] N. Lockyer *et al.*, *Phys. Rev. D* **30**, 860 (1984).
- [17] A.N. Zelenski *et al.*, in *Proceedings of the 12th International Symposium on High Energy Spin Physics (SPIN96)*, edited by C.W. de Jager *et al.*, (World Scientific, Amsterdam, 1997), p. 637.
- [18] A.N. Zelenski *et al.*, in *Proceedings of the 6th Conference on Intersections Between Particle and Nuclear Physics*, edited by T.W. Donnelly, AIP Conference Proceedings 412, New York, 1997, p.328.
- [19] C.D.P. Levy *et al.*, in *Proceedings of the International Workshop on Polarized Beams and Polarized Gas Targets* (Cologne, 1995), edited by H.P. gen. Schieck and L. Sydow (World Scientific, Singapore, 1996), p. 120; A.N. Zelenski, *ibid.*, p. 111.
- [20] R.B. Wiringa, *et al.*, *Phys. Rev. C* **51**, 38 (1995).
- [21] R. Machleidt, *Phys. Rev. C* **63**, 24001 (2001).
- [22] J.A. Carlson, R. Schiavilla, V.R. Brown, and B.F. Gibson, *Phys. Rev. C* **65**, 035502, (2002); R. Schiavilla, private communication (2001).
- [23] B. Desplanques, J.F. Donoghue, and B.R. Holstein, *Ann. Phys.(N.Y.)* **124**, 449 (1980).
- [24] W.M. Snow *et al.*, *Nucl. Inst. Meth. A* **440**, 729 (2000).
- [25] J.F. Caviagnac *et al.*, *Phys. Lett. B* **67**, 148 (1977).

- [26] J. Alberi *et al.*, Can. J. Phys. **66**, 542 (1988).
- [27] D. Beck, spokesperson, Jefferson Lab proposal E00-006 (2000).
- [28] E.J. Brash *et al.*, Phys. Rev. C **65**, 05100 (2002).
- [29] R. Hasty *et al.*, Science **290**, 2117 (2000).
- [30] D. Spayde *et al.*, Phys Rev. Lett. **84**, 1106 (2000).
- [31] K.A. Aniol *et al.*, Phys. Rev. Lett. **82**, 1096 (1999).
- [32] K.A. Aniol *et al.*, Phys. Lett. **B509**, 211 (2001) (1999).
- [33] K. Kumar, Jefferson Lab proposal E99-115 (1999)
- [34] D. Armstrong, Jefferson Lab proposal E00-114 (2000).
- [35] D. von Harrach, spokesperson, F.E. Maas, contact, MAMI experiment A4-01-93 (1993).
- [36] F.E. Mass *et al.*, in *Proceedings of Parity Violations in Atoms and Polarized Electron Scattering* (Paris, 1997), edited by B. Frois and M.A. Bouchiat (World Scientific, Singapore, 1999).
- [37] F.E. Maas, Eur. Phys. J. A **17**, 339 (2003).
- [38] G. Batigne in *Proceedings of the 4th International Conference on Perspectives in Hadronic Physics* (Trieste, 2003), G0 report G0-03-075, (this report and others are available from <http://www.npl.uiuc.edu/exp/G0/docs/>).